Validation of Molecular Docking Calculations Involving FGF-1 and FGF-2

Ian Bytheway* and Siska Cochran

Drug Design Group, Progen Industries Limited, 2806 Ipswich Rd, Darra, Queensland 4076, Australia

A predictive relationship between calculated and observed binding affinities for the complexation of ligands to the fibroblast growth factors FGF-1 and FGF-2 based on molecular docking calculations is described. The majority of the ligands examined in this study have high conformational flexibility, and to account for this, multiple conformers were generated for each and subsequently used in flexible docking calculations. Two scoring functions, Gscore and Emodel, were used to quantify the protein:ligand interaction of which the Emodel score showed the best correlation with experimental binding energies. Both scoring functions, however, predicted similar locations for the ligand sulfate groups in the binding site. The van der Waals radii of nonpolar atoms of both the protein and ligand, which modify the effective sizes of both the protein binding site and the ligand, were also systematically altered by factors of 1.0, 0.9, and 0.8 in order to optimize the conditions for predictive docking. Least squares analyses of the Emodel scores against experimental binding energies yielded best r^2 values of 0.91 and 0.83 for FGF-1 and FGF-2, respectively, with slightly lower q^2 values. Optimized scale factor combinations in conjunction with the least squares lines of best fit based on the Emodel function were used to define a predictive model that was tested against ligands not included in the original set. Acceptable predictions of binding affinity were obtained for use in the initial screening of potential leadlike molecules for both FGF-1 and FGF-2.

Introduction

Fibroblast growth factors (FGFs) have been implicated in several human angiogenic pathologies, and inhibition of angiogenesis as a therapeutic approach in the treatment of cancer was suggested over 30 years ago.[1] Anticancer agents that have been developed to target the FGFs include heparin-mimicking polysulfonated compounds,[2] suramin and the related suradistas,[3] and sulfated oligosaccharides.[4,5] There are no small molecule inhibitors of the FGFs in widespread clinical use as antiangiogenic agents, though recent studies using monosaccharides[6] and naphthalene sulfonate derivatives[7] demonstrate the promise of this approach. The work described in this paper is a part of our effort to design FGF inhibitors.

The FGFs are mediators of physiological development and morphogenesis. They function by binding to and dimerizing FGF receptors leading to receptor activation and subsequent cell signaling.[8–10] This process is facilitated in vivo through the binding of heparan sulfate to the FGFs, and the prevention of this interaction may form the basis for antiangiogenic therapies. For example, exogenous heparin efficiently competes with heparan sulfate for the FGFs and their receptors,[11] and recent three-dimensional structures of the heparin:FGF:FGFR ternary complex[12,13] suggest a central role for heparin in the stabilization of the FGF:FGFR complex.

Heparin and heparan sulfate are glycosaminoglycans (GAGs) of variable sequence and chain length based upon a repeating 1→4 linked D-glucosamine and uronic acid motif modified by differential sulfation, acetylation, and epimerization. Both molecules are large, with molecular weights ranging from 5 to 50 kDa, and highly negatively charged.[14,15] Molecules smaller than heparin or heparan sulfate also exhibit binding to the FGFs, and several experimental structures of both FGF-1 and FGF-2 complexed with smaller oligosaccharides are known. The sulfated disaccharide sucrose octasulfate (SOS) binds in the heparin binding site of FGF-1[16] and mimics the natural heparan sulfate ligand by promoting the formation of the FGF-2:FGFR-1:SOS ternary complex.[17] NMR studies of naphthalene trisulfonate (NTS)[18] complexed with FGF-1 showed that NTS binds in the same site as heparin.[19] An X-ray crystal structure of a monosulfonated naphthalene derivative complexed with FGF-1 also demonstrates that molecules with much less complexity than heparin can bind and inhibit FGFs.[7]

The size and conformational flexibility of the oligosaccharide ligands that are native to the FGFs are the major challenges confronting the molecular modeling of FGF:ligand complexes. Reduction in the size of the native ligand to include only those sugar units involved in FGF binding is often a necessary concession. Calculations[20,21] of a pentasaccharide binding to FGF-2 using a combination of rigid manual docking, energy minimization, and molecular dynamics simulation demonstrated that an oligosaccharide fragment could be used to model the binding of heparan sulfate to FGF-2. These studies also showed that the protein residues interacting most strongly with the pentasaccharide agreed with the mode of binding anticipated from site-directed mutagenesis studies. Rigid manual docking was also used to examine the binding of a hexasaccharide to FGF-2 in a study of the activation of FGF-2 by sulfated colominic acid.[22]

Conformational flexibility inherent in oligosaccharide systems might also be profitably reduced to an accept-

* To whom correspondence should be addressed. Tel: (61-7) 3273 9184. Fax: (61-7) 3375 6746. E-mail: Ian.Bytheway@progen.com.au.

able level by considering experimentally derived conformations in conjunction with rigid docking calculations. This approach was used to show how a heparin-derived pentasaccharide could mimic the natural ligand and also enabled prediction of the heparin binding site in FGF-2.[23] Docking of oligosaccharides comprised of as many as 14 monosaccharides in conformations derived from experiment also proved useful in the study of chemokine:GAG binding.[24,25]

Flexible docking of a hexasaccharide ligand to both FGF-1 and FGF-2 has also been reported.[26] This study surveyed a range of flexible docking methodologies and showed that mono- and disaccharides derived from heparin or heparan sulfate can be used to probe heparin-binding residues without requiring more complex calculations involving the hexasaccharide ligand.[26] These results, along with the experimental findings that synthetic heparin-derived di- and trisaccharides,[27] SOS,[16] NTS,[18] and related molecules[7] bind to the same binding site occupied by heparin, are important factors in developing inhibitors and suggest potential therapies that might limit angiogenesis.

Despite these findings, the exploration of FGF binding sites by computational methods is not common since the calculations are generally too demanding for routine studies. This is understandable given the size and degree of conformational complexity of the natural ligands for the FGFs, and their derivatives, as such molecules are at the upper end or beyond the limits usually applied during routine in silico screening. Furthermore, such large and flexible molecules are not readily envisaged as viable drug candidates.[28,29] Computational studies of FGF binding are also complicated by the location of the heparin binding site on the surface of these proteins[30] which compounds the problem of conformational flexibility by effectively offering the ligand less binding constraints. In this way the shallow FGF binding sites differ from the deeper pockets often explored in protein:ligand binding, for example in algorithm validation[31] or scoring function comparison.[32]

The work described here is concerned with the development of strategies for performing docking calculations using flexible ligands to examine the heparin binding sites of FGF-1 and FGF-2. Central to the success or otherwise of these calculations are experimental binding data which have been used to determine optimal parameters for docking calculations and the appropriateness of scoring functions.

Computational Details

The X-ray crystal structures of FGF-1 and FGF-2 (pdb accession codes 1AFC[16] and 1BFB,[33] respectively) used to model the protein structures in this study both contain bound ligands that define the relevant binding sites: sucrose octasulfate in FGF-1 and a heparin-derived tetrasaccharide in FGF-2. Water molecules of crystallization were removed from the complexes, and the proteins prepared for docking using the protein preparation utility provided by Schrödinger LLC and the Impact[34] program (FirstDiscovery v2.5). During this preparation process, basic residues in the region of the binding site were protonated to give octapositive formal charge and a protein:ligand complex with overall neutral charge. Cavity radii defining the region of the binding site considered during the protonation step were 10.48 Å for FGF-1 and 18.4 Å for FGF-2. Partial atomic charges were assigned according to the OPLS-AA force field.[35]

All docking calculations were performed using the Glide program (FirstDiscovery v2.5) and the 2001 implementation of the OPLS-AA force field.[35] The binding site, for which the various energy grids were calculated and stored, is defined in terms of two concentric cubes: the bounding box, which must contain the center of any acceptable ligand pose, and the enclosing box, which must contain all ligand atoms of an acceptable pose. Cubes with an edge length of 14 Å and centered at the midpoint of the longest atom−atom distance in the respective cocrystallized ligands defined the bounding boxes in both proteins. The larger enclosing boxes were also defined in terms of the cocrystallized ligands: edge lengths of 28 and 33.8 Å were used for FGF-1 and FGF-2, respectively.
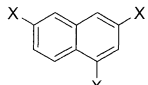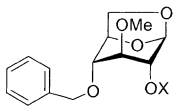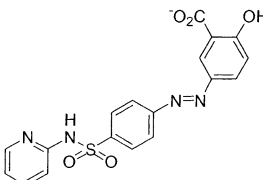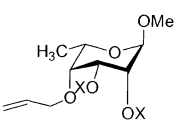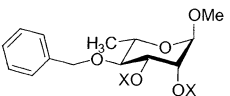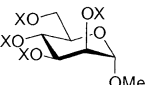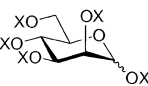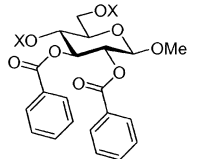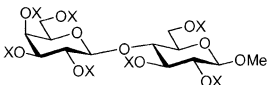
Default input parameters were used in all of the docking calculations with the exception of the *maxkeep* variable which sets the maximum number of poses generated during the initial phase of the docking calculation that are passed to the energy minimization step. In these calculations *maxkeep* was increased to 800, compared to the default value of 400. Upon completion of each docking calculation one pose per ligand was saved.

Glide's primary scoring function is GlideScore (abbreviated as Gscore). It is a modified and extended version of the empirically based ChemScore function[36] and recent studies[37] predicted binding affinities to within a root-mean-square deviation (rmsd) of 2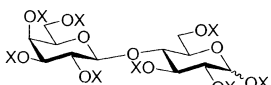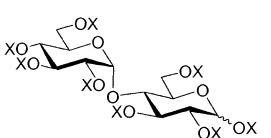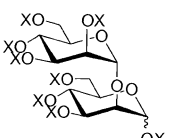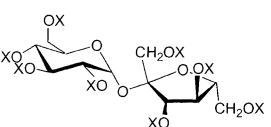.3 kcal/mol when compared with experiment. Our initial studies, however, suggested that Gscore did not correlate with experimental binding affinities all that well and another scoring function used by Glide, Emodel, was explored. The Emodel function is itself derived from a combination of the Gscore, Coulombic, and van der Waals energies and the strain energy of the ligand.[37]

Scale factors that reduce the van der Waals radii of nonpolar atoms of both the protein and ligand are incorporated into Glide. These effectively make the binding site larger and the ligand smaller, and lower the energy penalties associated with close protein:ligand contacts. Such scaling is intended to mimic the changes that might occur in a binding site upon ligand complexation, and modification of scale parameters, therefore, allows for optimization of docking calculations within Glide. Scaling was applied to those atoms with absolute partial charges less than or equal to 0.15 and 0.25 electrons for protein and ligand atoms, respectively, in accordance with standard Glide definitions. Scale factors of 0.8, 0.9, and 1.0 were applied systematically to the FGF−(1,2):ligand complexes, resulting in nine separate docking calculations for each protein:ligand complex. Scale factor combinations are denoted scale(protein)/scale(ligand) throughout, thus "0.8/0.9" denotes calculations performed with a scale factor of 0.8 for nonpolar protein atoms (|partial charge| ≤ 0.15 e) and 0.9 for nonpolar ligand atoms (|partial charge| ≤ 0.25 e).

Relatively few computational studies of the binding of small molecules to FGFs have been carried out, and none have involved the determination of protein:ligand binding energies for direct comparison with experimental values. To calibrate the docking methodology described here with experiment, ligands with known binding energies and a degree of torsional flexibility capable of treatment by Glide were required. Molecules satisfying these criteria were taken from both commercially available (naphthalene trisulfonate, **1**; sulfasalazine, **2**; and sucrose octasulfate, **3**) and recently synthesized molecules[38,39] for which experimental binding affinities had been measured using a surface plasmon resonance-based solution affinity assay.[40] The ligands used in this study, along with their averaged experimental binding affinities[41] to FGF-1 and FGF-2, are shown in Table 1. Where mixtures of both α- and β-anomeric forms of a ligand were assayed (ligands **7**, **10**, **11**, and **12** in Table 1) calculations were performed for both anomers, and the same experimental dissociation constant (K_d) was given to both and subsequently used in the statistical analyses. Although this procedure adds uncertainty to the statistical analyses, it is preferable that some attempt to account for this situation be made as the procedure described here is intended for use when anomeric purity is not assured.

Table 1. Chemical Structures of the Ligands Used to Determine Appropriate Scale Factor Combinations for Use in Docking Calculations[a]

Ligand		N_r	N_c	FGF-1		FGF-2	
				K_d	ΔG[b]	K_d	ΔG[b]
1		3	1	474	-4.53	223	-4.98
2		6	2	307	-4.79	8020	-2.86
3		7	4	609	-4.38	None Observed	-
4		8	3	1340	-3.92	None Observed	-
5		8	1	337.5	-4.73	249	-4.91
6		10	5	127	-5.31	343	-4.72
7		11	3 (α) 10 (β)	37.5	-6.04	155	-5.19
8		12	4	921	-4.14	None Observed	-
9		19	93	1.15	-8.10	16.2	-6.53
10		20	41 (α) 33 (β)	1.2	-8.07	13.3	-6.65
11		20	101 (α) 101 (β)	0.54	-8.54	6.3	-7.09
12		20	19 (α) 65 (β)	0.13	-9.39	26.7	-6.24
13		21	140	0.74	-8.36	5.5	-7.17

[a] X denotes the SO_3^- functional group; N_r is the number of rotatable bonds in the ligand; N_c is the number of conformers used as input for docking calculations; K_d is the experimentally observed dissociation constant in units of μM; and ΔG is the corresponding binding affinity in units of kcal/mol. [b] $\Delta G = RT \ln K_d$, $T = 298$ K.

Table 2. Values of r^2 and q^2 for the Comparison of Gscore and Emodel Scoring Functions Obtained from the Glide Docking Calculations with Experimental Binding Affinities[a]

scale factors	FGF-1				FGF-2			
	Gscore		Emodel		Gscore		Emodel	
	r^2	q^2	r^2	q^2	r^2	q^2	r^2	q^2
0.8/0.8	0.68	0.61	0.87	0.84	0.69	0.55	0.83	0.73
0.8/0.9	0.59	0.48	0.91	0.88	0.66	0.54	0.81	0.70
0.8/1.0	0.58	0.49	0.90	0.87	0.51	0.38	0.76	0.64
0.9/0.8	0.42	0.31	0.88	0.85	0.40	0.26	0.82	0.72
0.9/0.9	0.61	0.46	0.89	0.86	0.53	0.40	0.78	0.66
0.9/1.0	0.60	0.52	0.90	0.87	0.61	0.44	0.81	0.69
1.0/0.8	0.48	0.39	0.89	0.86	0.53	0.35	0.83	0.73
1.0/0.9	0.67	0.60	0.88	0.85	0.52	0.35	0.82	0.71
1.0/1.0	0.41	0.29	0.89	0.86	0.62	0.47	0.79	0.67

[a] r^2 is the squared correlation coefficient derived from the linear regression analysis, and q^2 is the squared correlation coefficient derived from the leave-one-out analysis. Scale factors are shown as scale(protein)/scale(ligand) pairs.

Although much smaller than the native heparan sulfate ligand that binds to these growth factors in vivo, the ligands shown in Table 1 average nearly 14 rotatable bonds per molecule and are more flexible than those typically examined in docking studies.[42−44] Such flexibility increases both the effort required to generate bioactive ligand conformations[45,46] and the possibility that regions of conformational space may not be sampled properly.[43]

To compensate for the excessive ligand flexibility encountered in this study a set of conformers was generated for each ligand using the Monte Carlo multiple minimum (MCMM) conformational search algorithm[47] in conjunction with the OPLS-AA force field and the GB/SA solvent model[48] as implemented in the MacroModel program (v8.0, v8.1).[49] The relatively rigid ligands (having less than 12 rotatable bonds) were subjected to a 1000-step conformational search while for the remaining ligands a conformational search was performed with the number of Monte Carlo steps equal to 500 times the number of rotatable bonds. Only those conformers within 6 kcal/mol of the global minimum were kept and the Xcluster[50] program was used to find a manageable number of representative conformations for each ligand. The number of conformers docked for each ligand is given in Table 1. This approach is similar to both the "divide and conquer" methodology for treating flexible ligands[51] and a recent docking study of a large and flexible peptide ligand.[52]

Linear regression and cross-validation analyses were performed using the MARTHA pattern recognition software.[53,54] The Fisher F statistic[55] calculated during the course of the linear regression analyses was used to test the significance of the squared correlation coefficients (r^2 and q^2). F values for all regression analyses are included in the Supporting Information.

Results and Discussion

Scale Factor Selection. The ligand conformations that gave the lowest, or "best", Gscore and Emodel values for each scale factor combination were compared with the experimental binding energies. The r^2 values from the regression analyses for all scale factor combinations are given in Table 2. The Emodel-derived r^2 values are uniformly higher than the corresponding Gscore values, suggesting that Emodel is a better descriptor of binding affinity for these FGF:ligand complexes. Also shown in Table 2 are the q^2 values obtained from a leave-one-out analysis of each data set. The q^2 values based on the Emodel results for both FGFs suggest a reasonable goodness-of-prediction, while for the Gscore data the predictivity is somewhat lower. Fisher F values indicate significance at the 95% confi-
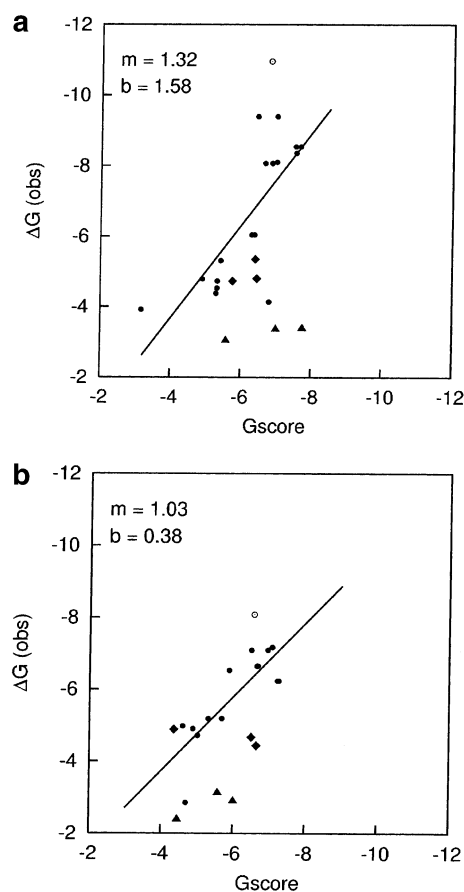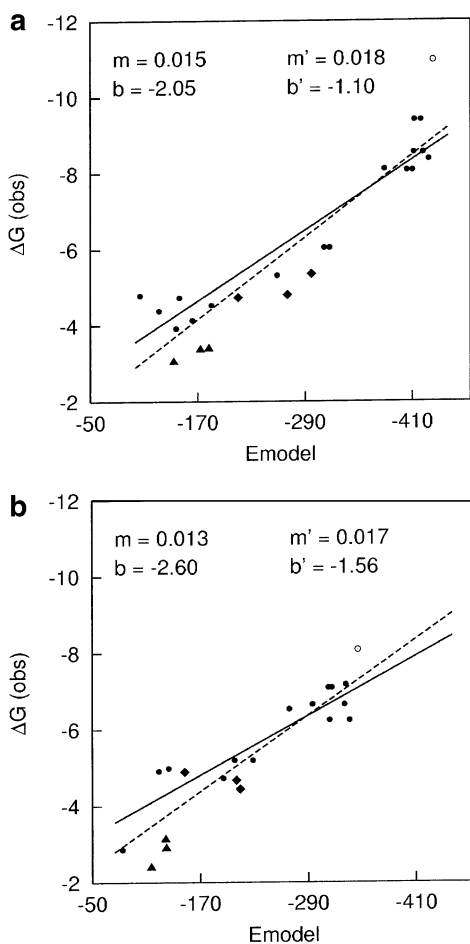

Figure 1. Plots of experimental ΔG values against calculated Gscore values. (a) FGF-1 calculated using the 0.8/0.9 scale factor combination, (b) FGF-2 calculated using the 0.8/0.8 scale factor combination. All energies are given in units of kcal/mol. The ligands in Table 1 are denoted by filled circles, an open circle denotes **14**, filled triangles denote ligands **15−17**, and filled diamonds denote ligands **18−20**. The least squares lines of best fit, with gradient m and y-intercept b, calculated using ligands **1−13** (Table 1) are also shown.

dence interval[56] for all regression analyses while significance at the 99% confidence interval is indicated for all but the lowest r^2 and q^2 values in Table 2.

The r^2 values obtained from the regression analyses given in Table 2 indicate that the majority of scale factor combinations produce acceptable agreement with experiment when using the Emodel scoring function, while greater variation in the range of r^2 values is found for comparisons with the Gscore function. The scale factor combinations chosen, therefore, were those that, in the first instance, performed best for the Emodel function followed by the performance of the Gscore function. This resulted in the choice of the 0.8/0.9 scale factor combination for FGF-1 and 0.8/0.8 for FGF-2.

Plots of the experimental binding energies against Gscore and Emodel obtained from the docking calculations that used the optimal scale factor combinations, along with their corresponding least squares lines, are shown in Figures 1 and 2. While correlation between Gscore and the experimental binding energies is low (Figure 1), agreement between Emodel and experiment is significantly better (Figure 2). In the case of FGF-1 there are several discrepancies between the experimental binding energies and Gscore values that are not present in the corresponding Emodel plot. For FGF-2

Figure 2. Plots of experimental ΔG values against calculated Emodel values. (a) FGF-1 calculated using the 0.8/0.9 scale factor combination, (b) FGF-2 calculated using the 0.8/0.8 scale factor combination. All energies are in kcal/mol. Ligands are denoted using the same symbols described in Figure 1. The least squares lines of best fit, with gradient m and y-intercept b, calculated using ligands **1**−**13** (Table 1) are shown as full lines. The least squares lines of best fit, with gradient m' and y-intercept b', calculated using ligands **1**−**20** are shown as dashed lines.

there is one significant outlier in both plots, **2**, which has the lowest measured binding affinity. Both scoring functions predict greater FGF-2 binding affinity for this ligand, though the Emodel prediction is slightly better than that of Gscore.

Influence of Scale Factor on Ligand Conformation. The best Emodel poses for all ligands obtained from calculations performed with 1.0/1.0 (i.e., no scaling of nonpolar van der Waals radii) and 0.8/0.8 scale factors are overlaid in Figure 3. An important feature of this figure is the general clustering of ligand positions within the binding site that is independent of the scale factors used. Ligands docked with FGF-1 show general clustering in the middle of the bounding box (which must contain the center of every ligand, see the Computational Details section above) that defines the binding site (Figure 3a) while for FGF-2 a preference for the bottom right region of the binding site is observed for both scale factor combinations (Figure 3b).

Scale factor choices for these protein systems are, therefore, important for obtaining optimal agreement with experimental binding energies, but less so for finding the "best" pose for any given ligand. This is
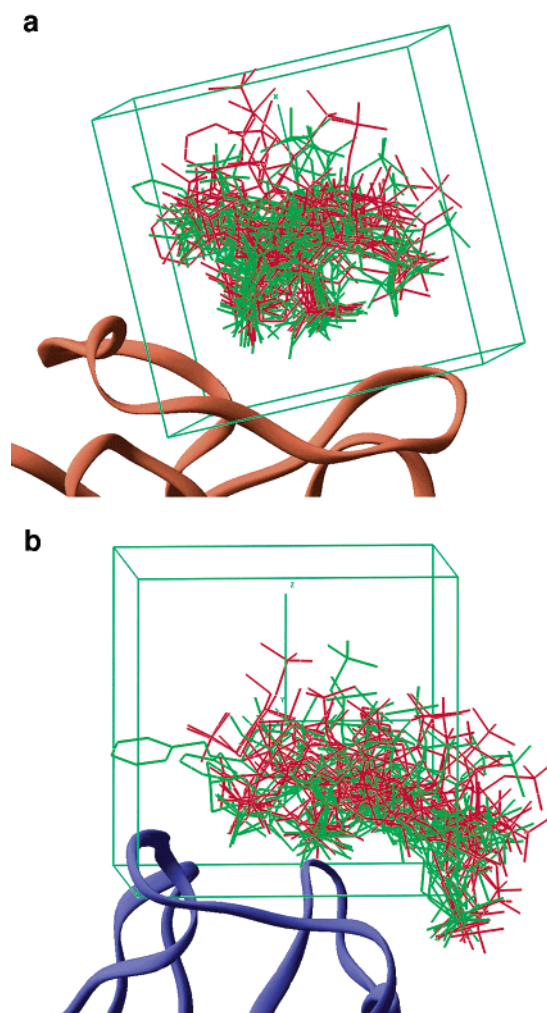
Figure 3. A comparison of the effect of scale factor choice on ligand conformation docked into (a) FGF-1 and (b) FGF-2. The best (lowest energy) Emodel poses obtained from 1.0/1.0 calculations are shown in red and those obtained from 0.8/0.8 calculations are shown in green. The protein backbones are depicted by ribbons and ligand hydrogen atoms are omitted. The binding site regions that must contain the ligand center during docking calculations are depicted by green cubes.

perhaps an unsurprising result as the binding site is quite open, by virtue of its situation on the protein surface, and the ligands are presented with only a face of the protein with which to bind. In this binding site ligands can be accommodated in much the same manner irrespective of small changes in the sizes of nonpolar van der Waals radii. This may not necessarily be the case, for example, in proteins where the binding site is more enclosed and size constraints more important.

Scoring Functions: Gscore Versus Emodel. Although better agreement with experiment is proffered by the Emodel scoring function, the conformations of the bound ligands predicted by the two scoring functions are in many cases the same (10 of 17 for FGF-1; 9 of 14 for FGF-2). Where binding conformations differ there is usually agreement in the positioning of the sulfate groups that bind to the protein. Examples are shown in Figure 4 for the complexes formed between FGF-1 and β-**12** (0.8/0.9 scaling) and FGF-2 and **6** (0.8/0.8 scaling) for which different Gscore and Emodel binding conformations are predicted. Although the modes of protein binding are different, both show similarly
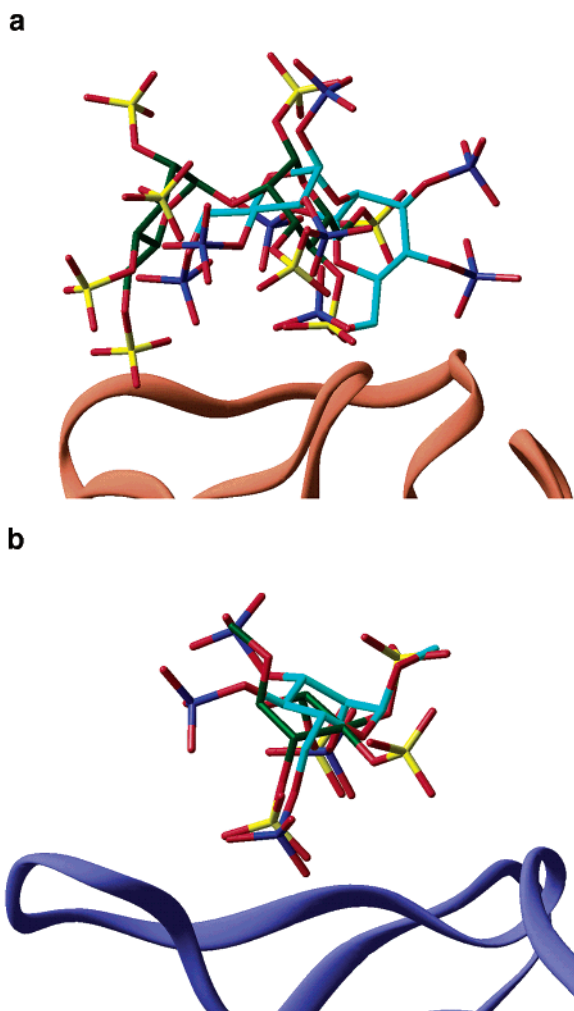
Figure 4. A comparison of the best Gscore (carbon = green, oxygen = red, sulfur = yellow) and Emodel (carbon = light blue, oxygen = red, sulfur = dark blue) poses calculated for (a) the FGF-1:β-**12** complex and (b) the FGF-2:**6** complex. Protein backbone atoms in both plots are depicted by ribbons.

positioned sulfate groups in the binding site. The rmsd between the two β-**12** conformations in Figure 4a, based on non-hydrogen atoms only, is 5.4 Å though sulfate groups clearly overlap. Similarly, Figure 4b shows clear overlap of two sulfate groups in the two docked conformations of **6** while the rmsd between the two poses is 6.6 Å.

The general similarity of Gscore and Emodel solutions to the docking problem suggests that there are no clear differences or preferences for one scoring function over the other: both may provide plausible conformations for the complexed ligands. This similarity, along with Emodel's overall better agreement with experimental binding energies, suggests that this scoring function is appropriate for these FGF systems, particularly as some degree of predictivity is required when screening possible lead candidates.

Sulfate Positions: Cocrystallized versus E-model. The docked poses displayed in Figures 3 and 4 suggest clustering of ligand sulfate groups in specific regions within the heparin binding sites. The validity of such clustering, as predicted by the Emodel function, is further explored in Figure 5 by comparing calculated sulfate positions with those observed in various struc-
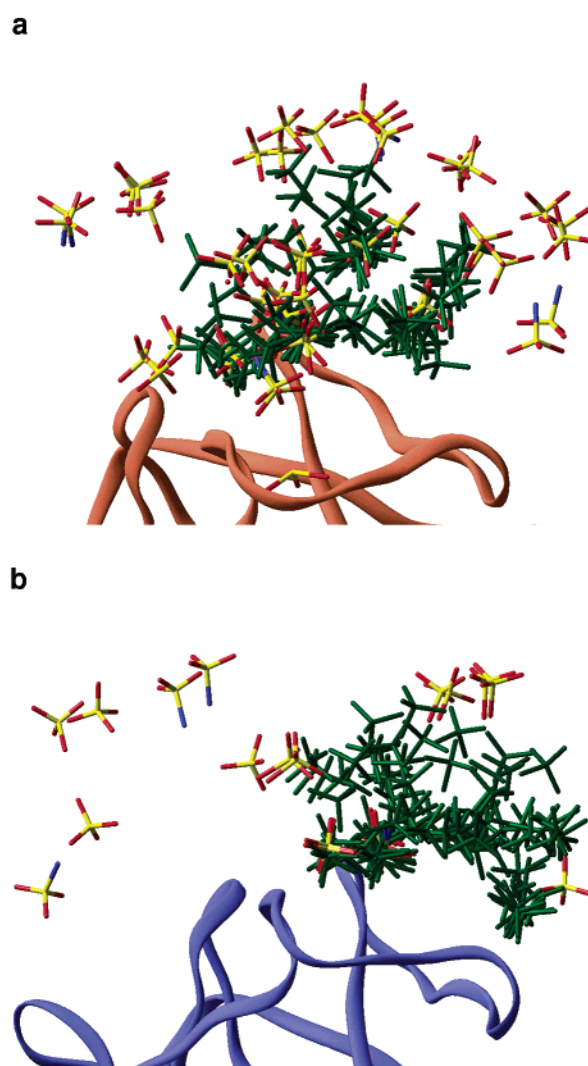
Figure 5. The positions of sulfate groups from ligands predicted by the Emodel scoring function in conjunction with 0.8/0.9 and 0.8/0.8 scaling for FGF-1 and FGF-2, respectively. Also shown are the relative positions observed for sulfate groups of cocrystallized ligands (including sulfate ions) in the different crystal structures available for FGF-1 and FGF-2. Predicted ligand sulfate groups are shown in green while cocrystallized *O*-sulfate and *N*-sulfate groups are colored according to the scheme: nitrogen = blue, oxygen = red, sulfur = yellow. (a) FGF-1 showing ligands from 1AFC, 1AXM, 1JT3, 1JT5, 1JT7, 1RML, and 2AXM. (b) FGF-2 showing ligands from 1BFB, 1BFC, 2FGF, 4FGF, and 1FGA.

ture determinations of FGF:ligand complexes. In Figure 5 the different cocrystallized protein:ligand complexes were aligned by their protein backbone atoms, and only the positions of the ligand sulfo functional groups (including cocrystallized sulfate ions) are shown. Where dimeric structures were observed in the crystal structure two protein:ligand monomer complexes were constructed and included in the superposition process. Our findings concur with those of Pellegrini[57] who also showed that the spatial overlap of sulfate groups of heparin fragments cocrystallized with FGFs is significant.

Figure 5 shows both the variety of sulfate positions in the binding site regions of FGF-1 and FGF-2 as well as their specificity. Qualitative agreement between observed and calculated sulfate positions is clear for

Table 3. Predicted Binding Affinities for Complexes of FGF-2 for Which Binding Was Not Experimentally Observed[a]

	Gscore	K_d	ΔG (Gscore)	K_d (Gscore)	Emodel	ΔG (Emodel)	K_d (Emodel)
3	−4.61	416	−4.36	632	−100.45	−3.90	1369
4	−5.03	205	−4.80	304	−119.53	−4.15	902
8	−5.91	46	−5.70	66	−122.20	−4.19	851

[a] Values of ΔG(Gscore), ΔG(Emodel), and the corresponding K_d values were derived from the least squares lines shown in Figures 1b and 2b. Energies are in kcal/mol and K_d values are in μM.

both FGFs, with the results for FGF-1 showing overlap of sulfates in the central region of the binding site. For FGF-2 it is interesting to note the tendency for sulfate groups to cluster toward the bottom right-hand region of the bounding box shown in Figure 3b, close to the side chain residues Asp80, Lys130, and Thr122. This has some experimental justification as a sulfate ion (from the structure with pdb accession code 2FGF) is also located in this region of the binding site (see Figure 5b). Presumably this region is not accessible to the larger oligosaccharide ligands but might be exploited by smaller charged groups such as a free sulfate ion or the ligands used in this study.

Implications for Screening. The ultimate aim of this study is to provide a reliable quantitative measure of binding affinities for FGF:ligand complexes. Although such measures may only be useful to within approximately 2 kcal/mol it would, of course, be helpful if promising candidates were identified for further investigation ahead of those unlikely to warrant extra attention.

The predictivity of the approach described here can be tested in the first instance by examining ligands **3**, **4**, and **8** for which binding to only FGF-1 was observed. Gscore and Emodel functions for these ligands docked with FGF-2 using the 0.8/0.8 scale factor combination along with the appropriate predicted binding affinities and K_d values are shown in Table 3. Gscore values obtained directly from the docking calculation suggest that all three ligands should bind to FGF-2 with binding affinities of between −5 and −6 kcal/mol ($K_d \approx 40-400$ μM), and predictions based on the least-squares fit of Gscore to observed ΔG values are similar. The least-squares fit using the Emodel data, however, suggests lower affinities of between −3.9 and −4.2 kcal/mol ($K_d \approx 850-1400$ μM). A prediction based on the Emodel scoring function and available binding data suggests, therefore, that these three ligands would, at best, bind only weakly to FGF-2.

Testing the Models. The predictive ability of the scoring functions for both FGFs was tested using the ligands in Table 4, and their calculated Gscore and Emodel values are also included in Figures 1 and 2. Of the ligands given in Table 4 only the experimental binding affinity of the polysulfated trisaccharide ligand **14** was known prior to commencing this study, thus **15**–**20** were used to test the utility of the lines of best fit shown in Figures 1 and 2 that relate docking scores to the measured K_d values.

The binding affinity of **14** was measured using a mixture of α- and β-anomers,[40] however, only the β-anomer was considered because of its high flexibility (29 rotatable bonds) and the computational effort required for both MCMM searching and the subsequent

docking of multiple input conformations. The best Gscore values calculated for β-**14** were −6.81 and −6.56 kcal/mol for FGF-1 and FGF-2, respectively, which are considerably lower than those observed, −11.05 (FGF-1) and −8.08 (FGF-2) kcal/mol. While it is clear that Gscore predicts moderate binding for this ligand to both FGFs, its affinity is underestimated possibly because of the large number of rotatable bonds in this molecule which incurs a penalty during the calculation of the Gscore.[37]

Emodel-derived binding affinities for β-**14** are closer to the observed values. The least squares line of best fit derived for the Emodel function for FGF-1 using the 0.8/0.9 scale factor combination predicted a binding affinity of −8.70 kcal/mol for β-**14**. The analogous least squares line of best fit for FGF-2 using the 0.8/0.8 scale factor combination predicted a binding affinity of −7.07 kcal/mol. Use of the Emodel scoring function in this manner, therefore, predicts binding between β-**14** and the FGFs that is stronger than anticipated on the basis of the Gscore function alone.
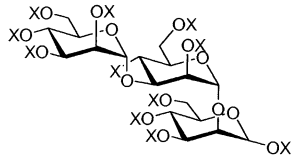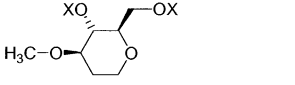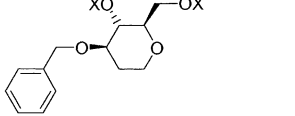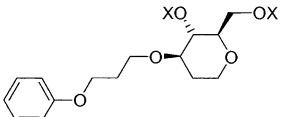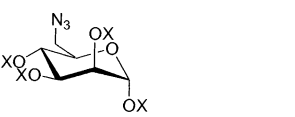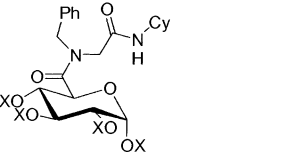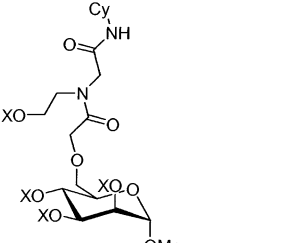
Gscore values for **15**−**17** binding to FGF-1 predict reasonable binding ranging from −5.6 to −7.8 kcal/mol (less than 100 μM), compared to the observed values of about −3.0 kcal/mol (approximately 3−6 mM), and appear as outliers in Figure 1a. The Emodel scores for the ligands **15**−**17**, however, are in better agreement with the proposed relationship between it and the observed binding affinity. The binding to FGF-1 predicted by Emodel for these ligands using the line of best fit given in Figure 2a is at the lower end of the series, with predictions based on the least-squares fit ranging from −4.2 to −4.8 kcal/mol, approximately l.2 to 1.5 kcal/mol stronger than observed. The over-estimation predicted using the Gscore least squares relationship shown in Figure 1a, on the other hand, is of the order of 3 to 5 kcal/mol.

The binding of **15**−**17** to FGF-2 shows similar trends, although their binding affinities for this protein are generally lower than those observed for FGF-1. The raw Gscore values predict binding energies ranging from −4.5 to −6.0 kcal/mol, and the least squares predictions are similarly better, compared to the observed binding energies of −2.4 to −3.1 kcal/mol. As with FGF-1, the Gscore function significantly over-estimates the binding affinities of these ligands. The Emodel values, however, suggest that these ligands are at the lower end of the binding range with predictions based on the least-squares fit for binding of the order of −4.1 to −4.3 kcal/mol for **15**−**17**.

The ligands **18**−**20** were also used to examine the predictivity of the least squares lines of best fit. As shown in Figures 1 and 2 both scoring functions predict that these ligands will bind moderately well, in accord with experiment. The Gscores for both FGFs are within 0.5 to 2.2 kcal/mol of the observed values, with an average unsigned difference of 1.4 kcal/mol. The least squares line derived from the Emodel function predicts binding affinities to within 0.3 to 1.2 kcal/mol of the observed values, with an average unsigned difference of 0.9 kcal/mol.

Although the Gscore and Emodel functions differ in their agreement with the observed binding affinities, the orientation of the ligands in the FGF binding sites

Table 4. Chemical Structures of the Ligands Used to Test the Least Squares Lines of Best Fit Derived for FGF-1 and FGF-2[a]

Ligand	N_r	N_c	FGF-1		FGF-2	
			K_d	ΔG^b	K_d	ΔG^b
14	29	100	0.0078	-11.05	1.18	-8.08
15	6	6	5940	-3.04	17400	-2.39
16	8	15	3410	-3.36	5100	-3.13
17	11	42	3250	-3.39	7500	-2.90
18	9	15	340	-4.73	258	-4.89
19	16	12	120	-5.35	375	-4.67
20	20	33	300	-4.80	550	-4.44

[a] See Table 1 for definitions. Cy and Ph are used to abbreviate the cyclohexyl and phenyl functional groups, respectively. [b] $\Delta G = RT \ln K_d$, $T = 298$ K.

predicted by both functions are quite similar. This is illustrated in Figure 6 for ligands **15**−**17**. In the case of FGF-1 the sulfate groups of all three ligands overlap almost perfectly, and only **16** shows orientational differences, namely in the position of the benzyl group, between the Gscore and Emodel poses. Similarly, the overlap of sulfate groups in the FGF-2 poses is also significant. The exception for FGF-2 is again **16**, for which the position of one sulfate group is conserved between scoring functions while the other sulfate group interacts with different side chain residues.

The orientational differences observed in **18**−**20** are similar. For both **18** and **20** there is little difference between the best Gscore and Emodel poses, while for **19** different modes of interaction with side chain residues are found. These results, along with those for **15**−**17**, further illustrate the point that the requirements for the positioning of sulfate groups in the FGF binding sites is quite specific, while those governing the orientation of other portions of the ligand are not.

Extending the Model. Addition of the ligands **14**−**20** to the original set (i.e., ligands **1**−**13**) is another test of the robustness of the least squares analyses for these FGF systems, as the predictive relationships already discussed should, of course, persist upon addition of more data. Inclusion of these ligands in the regression analyses of Gscore data for both FGFs, however, results in much reduced r^2 and q^2 values of 0.24 and 0.13 for FGF-1 and 0.42 and 0.31 for FGF-2. This is not surprising as the extra points, particularly **15**−**17**, increase the scatter in the plots dramatically (see Figure 1).

Predictions based on the Emodel function using all ligands are in keeping with the results obtained for **1**−**13**. For FGF-1 the r^2 and q^2 values obtained for all ligands are 0.86 and 0.83, respectively, and only slightly lower than the values obtained using the original set. Similarly, for FGF-2 the line of best fit determined using Emodel scores for all ligands gave r^2 and q^2 values of 0.82 and 0.78, respectively, similar to those already obtained for the original set. These least squares lines

a

b
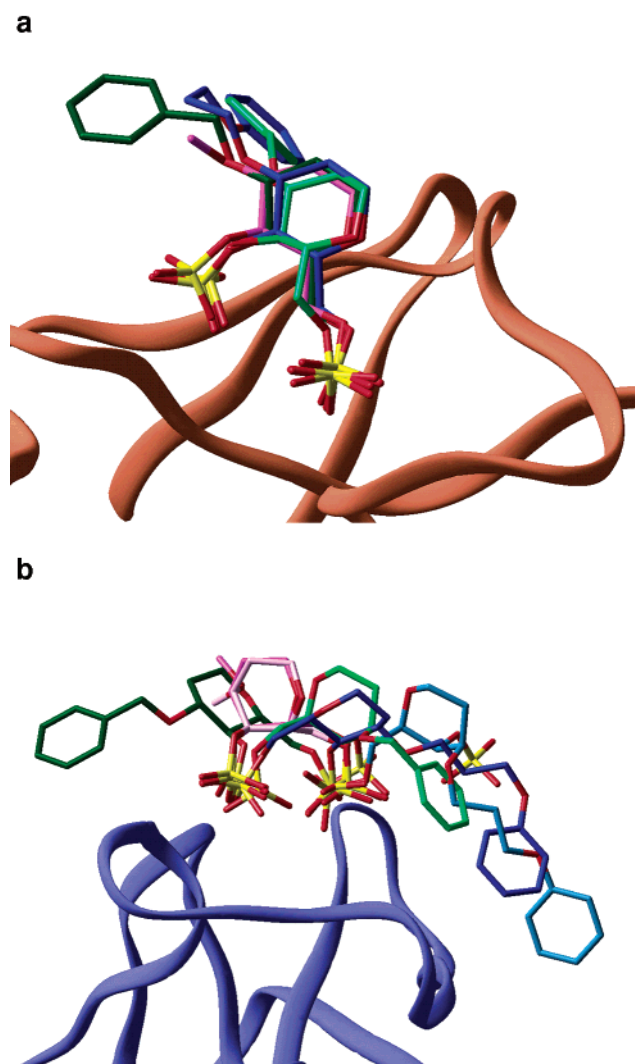
Figure 6. Comparison of Gscore and Emodel poses for **15**–**17** docked to (a) FGF-1 and (b) FGF-2. Atoms are colored according to red = oxygen and sulfur = yellow, while carbon atoms of the Gscore poses are colored: **15** = light purple, **16** = light green, and **17** = light blue. For the Emodel poses carbon atoms are colored: **15** = dark purple, **16** = dark green, and **17** = dark blue. The Gscore and Emodel poses of **15** and **17** in (a) are identical and only the Emodel coloring is shown.

of best fit calculated using all Emodel values are also shown in Figure 2a and b.

The inclusion of these extra ligands, which show strong, moderate and weak binding to FGF-1 and FGF-2, modifies the line of best fit by increasing both the gradient and the *y*-intercept (see Figure 2). While the relationship between the Emodel score and the measured binding affinity is preserved, the inclusion of more ligands, particularly those with stronger binding affinities, is required for the extension and continued utility of this approach for estimating FGF:ligand binding affinities.

Conclusions

The docking calculations described here show that the binding of charged ligands with FGF-1 and FGF-2 can be described semiquantitatively by the Emodel scoring function. This function predicts specificity in the binding site positions occupied by the ligand sulfate groups which correspond closely to the sulfate positions ob-

served in experimental structure determinations. The ligand positions predicted by the Gscore function are similar to those predicted by the Emodel function, particularly with respect to the orientation of sulfate groups, but do not show the same degree of correlation with experimental binding affinities.

The docking calculations described here were complicated by the open, surface nature of the binding site of the FGFs and by the very flexible nature of the ligands that bind in it. Some attempt to account for the nature of the binding site was made by scaling nonpolar atomic radii of protein and ligand atoms to 80 or 90% of their standard values in order to obtain the best agreement between observed binding energies and calculated docking scores. Although little variation in the agreement between Emodel and experiment was found over the range of scale factors considered, those chosen also maximized the performance of the Gscore function, hence their choice. Ligand flexibility was treated by performing the (flexible) docking calculations using a family of conformers for each ligand previously derived from conformational searching. Such an approach appears necessary when highly flexible ligands of the type described here are used in the docking calculations.

The predictive nature of the least squares lines relating experimental binding energies with Emodel and Gscore were tested against seven related molecules not used in the original statistical analyses. The predictions for six of these, based on the Emodel scoring function, suggested only weak to moderate binding, in accord with experiment. The semiquantitative nature of the relationship is clear, however, as predicted binding affinities were stronger than the observed values. Thus the model is probably most valuable in situations where Gscore is liable to predict strong binding at odds with experiment, while the correlation with Emodel appears more realistic.

The calculations described here show how the relatively complex problem of docking flexible ligands to a binding site on a protein surface might be tackled. Flexible docking involving multiple conformers per ligand, an appropriate scoring function and scaling of the nonpolar atoms involved in the binding event, suggest a methodology for the design of small molecule inhibitors for FGF-1 and FGF-2.

Supporting Information Available: Tables of calculated Gscore and Emodel values for all FGF:ligand complexes and regression data from the corresponding least squares analyses. This material is available free of charge via the Internet at http://pubs.acs.org.

References

(1) Folkman, J. Tumor Angiogenesis: Therapeutic Implications. *N. Engl. J. Med.* **1971**, *285*, 1182–1186.

(2) Liekens, S.; Leali, D.; Neyts, J.; Esnouf, R.; Rusnati, M.; Dell'Era, P.; Maudgal, P. C.; De Clercq, E.; Presta, M. Modulation of Fibroblast Growth Factor-2 Receptor Binding, Signaling, and Mitogenic Activity by Heparin-Mimicking Polysulfonated Compounds. *Mol. Pharmacol.* **1999**, *56*, 204–213.

(3) Sola, F.; Farao, M.; Pesenti, E.; Marsiglio, A.; Mongelli, N.; Grandi, M. Antitumor Activity of FCE 26644 a New Growth-Factor Complexing Molecule. *Cancer Chemother. Pharmacol.* **1995**, *36*, 217–222.

(4) Foxall, C.; Wei, Z.; Schaefer, M. E.; Casabonne, M.; Fugedi, P.; Peto, C.; Castellot, J. J.; Brandley, B. K. Sulfated Malto-Oligosaccharides Bind to Basic FGF, Inhibit Endothelial Cell Proliferation, and Disrupt Endothelial Cell Tube Formation. *J. Cell. Physiol.* **1996**, *168*, 657–667.

(5) Parish, C. R.; Freeman, C.; Brown, K. J.; Francis, D. J.; Cowden, W. B. Identification of Sulfated Oligosaccharide-Based Inhibitors of Tumor Growth and Metastasis Using Novel *in Vitro* Assays for Angiogenesis and Heparanase Activity. *Cancer Res.* **1999**, *59*, 3433–3441.

(6) Murphy, P. V.; Pitt, N.; O'Brien, A.; Enright, P. M.; Dunne, A.; Wilson, S. J.; Duane, R. M.; O'Boyle, K. M. Identification of Novel Inhibitors of Fibroblast Growth Factor (FGF-2) Binding to Heparin and Endothelial Cell Survival from a Structurally Diverse Carbohybrid Library. *Bioorg. Med. Chem. Lett.* **2002**, *12*, 3287–3290.

(7) Fernández-Tornero, C.; Lozano, R. M.; Redondo-Horcajo, M.; M. Gómez, A.; López, J. C.; Quesada, E.; Uriel, C.; Valverde, S.; Cuevas, P.; Romero, A.; Giménez-Gallego, G. Leads for Development of New Naphthalenesulfonate Derivatives with Enhanced Antiangiogenic Activity: Crystal Structure of Acidic Fibroblast Growth Factor in Complex with 5-amino-2-naphthalenesulfonate. *J. Biol. Chem.* **2003**, *278*, 21774–21781.

(8) Yayon, A.; Klagsbrun, M.; Esko, J. D.; Leder, P.; Ornitz, D. M. Cell Surface, Heparin-Like Molecules are Required for Binding of Basic Fibroblast Growth Factor to its High Affinity Receptor. *Cell* **1991**, *64*, 841–848.

(9) Rapraeger, A. C.; Krufka, A.; Olwin, B. B. Requirement of Heparan Sulfate for bFGF-Mediated Fibroblast Growth and Myoblast Differentiation. *Science* **1991**, *252*, 1705–1708.

(10) Ornitz, D. M.; Yayon, A.; Flanagan, J. G.; Svahn, C. M.; Levi, E.; Leder, P. Heparin is Required for Cell-Free Binding of Basic Fibroblast Growth Factor to a Soluble Receptor and for Mitogenesis in Whole Cells. *Mol. Cell. Biol.* **1992**, *12*, 240–247.

(11) Coltrini, D.; Rusnati, M.; Zoppetti, G.; Oreste, P.; Grazioli, G.; Naggi, A.; Presta, M. Different Effects of Mucosal, Bovine Lung and Chemically Modified Heparin on Selected Biological Properties of Basic Fibroblast Growth Factor. *Biochem. J.* **1994**, *303*, 583–590.

(12) Schlessinger, J.; Plotnikov, A. N.; Ibrahimi, O. A.; Eliseenkova, A. V.; Yeh, B. K.; Yayon, A.; Linhardt, R. J.; Mohammadi, M. Crystal Structure of a Ternary FGF–FGFR–Heparin Complex Reveals a Dual Role for Heparin in FGFR Binding and Dimerization. *Mol. Cell* **2000**, *6*, 743–750.

(13) Pellegrini, L.; Burke, D. F.; von Delft, F.; Mulloy, B.; Blundell, T. L. Crystal Structure of Fibroblast Growth Factor Receptor Ectodomain Bound to Ligand and Heparin. *Nature* **2000**, *407*, 1029–1034.

(14) Rabenstein, D. L. Heparin and Heparan Sulfate: Structure and Function. *Nat. Prod. Rep.* **2002**, *19*, 312–331.

(15) Capila, I.; Linhardt, R. J. Heparin-Protein Interactions. *Angew. Chem., Int. Ed.* **2002**, *41*, 391–412.

(16) Zhu, X.; Hsu, B. T.; Rees, D. C. Structural Studies of the Binding of the Anti-Ulcer Drug Sucrose Octasulfate to Acidic Fibroblast Growth Factor. *Structure* **1993**, *1*, 27–34.

(17) Yeh, B. K.; Eliseenkova, A. V.; Plotnikov, A. N.; Green, D.; Pinnell, J.; Polat, T.; Gritli-Linde, A.; Linhardt, R. J.; Mohammadi, M. Structural Basis for Activation of Fibroblast Growth Factor Signaling by Sucrose Octasulfate. *Mol. Cell. Biol.* **2002**, *22*, 7184–7192.

(18) Lozano, R. M.; Jiménez, M. Á.; Santoro, J.; Rico, M.; Giménez-Gallego, G. Solution Structure of Acidic Fibroblast Growth Factor Bound to 1,3,6-naphthalenetrisulfonate: A Minimal Model for the Anti-tumoral Action of Suramins and Suradistas. *J. Mol. Biol.* **1998**, *281*, 899–915.

(19) DiGabriele, A. D.; Lax, I.; Chen, D. I.; Svahn, C. M.; Jaye, M.; Schlessinger, J.; Hendrickson, W. A. Structure of a Heparin-Linked Biologically Active Dimer of Fibroblast Growth Factor. *Nature* **1998**, *393*, 812–817.

(20) Thompson, L. D.; Pantoliano, M. W.; Springer, B. A. Energetic Characterization of the Basic Fibroblast Growth Factor-Heparin Interaction: Identification of the Heparin Binding Domain. *Biochemistry* **1994**, *33*, 3831–3840.

(21) Pantoliano, M. W.; Horlick, R. A.; Springer, B. A.; Van Dyk, D. E.; Tobery, T.; Wetmore, D. R.; Lear, J. D.; Nahapetian, A. T.; Bradley, J. D.; Sisk, W. P. Multivalent Ligand–Receptor Binding Interactions in the Fibroblast Growth Factor System Produce a Cooperative Growth Factor and Heparin Mechanism for Receptor Dimerization. *Biochemistry* **1994**, *33*, 10229–10248.

(22) Kunou, M.; Koizumi, M.; Shimizu, K.; Kawase, M.; Hatanaka, K. Synthesis of Sulfated Colominic Acids and their Interaction with Fibroblast Growth Factors. *Biomacromolecules* **2000**, *1*, 451–458.

(23) Mulloy, B.; Forster, M. J. Conformation and Dynamics of Heparin and Heparan Sulfate. *Glycobiology* **2000**, *10*, 1147–1156.

(24) Sadir, R.; Baleux, F.; Grosdidier, A.; Imberty, A.; Lortat-Jacob, H. Characterization of the Stromal Cell-Derived Factor-1α–Heparin Complex. *J. Biol. Chem.* **2001**, *276*, 8288–8296.

(25) Lortat-Jacob, H.; Grosdidier, A.; Imberty, A. Structural Diversity of Heparan Sulfate Binding Domains in Chemokines. *Proc. Natl Acad. Sci. U.S.A.* **2002**, *99*, 1229–1234.

(26) Bitomsky, W.; Wade, R. C. Docking of Glycosaminoglycans to Heparin-Binding Proteins: Validation for aFGF, bFGF, and Antithrombin and Application to IL-8. *J. Am. Chem. Soc.* **1999**, *121*, 3004–3013.

(27) Ornitz, D. M.; Herr, A. B.; Nilsson, M.; Westman, J.; Svahn, C. M.; Waksman, G. FGF Binding and FGF Receptor Activation by Synthetic Heparan-Derived Di- and Trisaccharides. *Science* **1995**, *268*, 432–436.

(28) Lipinski, C. A.; Lombardo, F.; Dominy, B. W.; Feeney, P. J. Experimental and Computational Approaches to Estimate Solubility and Permeability in Drug Discovery and Development Settings. *Adv. Drug Delivery Rev.* **1997**, *23*, 3–25.

(29) Veber, D. F.; Johnson, S. R.; Cheng, H.-Y.; Smith, B. R.; Ward, K. W.; Kopple, K. D. Molecular Properties that Influence the Oral Bioavailability of Drug Candidates. *J. Med. Chem.* **2002**, *45*, 2615–2623.

(30) Qasba, P. K. Involvement of Sugars in Protein–Protein Interactions. *Carbohydr. Polym.* **2000**, *41*, 293–309.

(31) Nissink, J. W. M.; Murray, C.; Hartshorn, M.; Verdonk, M. L.; Cole, J. C.; Taylor, R. A New Test for Validating Predictions of Protein–Ligand Interactions. *Proteins* **2002**, *49*, 457–471.

(32) Wang, R.; Lu, Y.; Wang, S. Comparative Evaluation of 11 Scoring Functions for Molecular Docking. *J. Med. Chem.* **2003**, *46*, 2287–2303.

(33) Faham, S.; Hileman, R. E.; Fromm, J. R.; Linhardt, R. J.; Rees, D. C. Heparin Structure and Interactions with Basic Fibroblast Growth Factor. *Science* **1996**, *271*, 1116–1120.

(34) Banks, J.; Cao, Y.; Damm, W.; Friesner, R.; Gallichio, E.; Halgren, T.; Levy, R.; Mainz, D.; Murphy, R. *Impact* 2.5; Schrödinger LLC: Portland.

(35) Jorgensen, W. L.; Maxwell, D. S.; Tirado-Rives, J. Development and Testing of the Opls All Atom Force Field on Conformational Energetics and Properties of Organic Liquids. *J. Am. Chem. Soc.* **1996**, *118*, 11225–11236.

(36) Eldridge, M. D.; Murray, C. W.; Auton, T. R.; Paolini, G. V.; Mee, R. V. Empirical Scoring Functions: I. The Development of a Fast Empirical Scoring Function to Estimate the Binding Affinity of Ligands in Receptor Complexes. *J. Comput.-Aided Mol. Des.* **1997**, *11*, 425–445.

(37) Schrödinger LLC. *FirstDiscovery Technical Notes*; Schrödinger Press: Portland, 2003.

(38) Fairweather, J. K.; Ferro, V. Unpublished results.

(39) Liu, L.; Ferro, V. Unpublished results.

(40) Cochran, S.; Li, C.; Fairweather, J. K.; Kett, W. C.; Coombe, D. R.; Ferro, V. Probing the Interactions of Phosphosulfomannans with Angiogenic Growth Factors by Surface Plasmon Resonance. *J. Med. Chem.* **2003**, *46*, 4601–4608.

(41) Li, C.; Cochran, S.; Ferro, V. Unpublished results.

(42) Stahl, M.; Rarey, M. Detailed Analysis of Scoring Functions for Virtual Screening. *J. Med. Chem.* **2001**, *44*, 1035–1042.

(43) Schulz-Gasch, T.; Stahl, M. Binding Site Characteristics in Structure-Based Virtual Screening: Evaluation of Current Docking Tools. *J. Mol. Mod.* **2003**, *9*, 47–57.

(44) Smith, R.; Hubbard, R. E.; Gschwend, D. A.; Leach, A. R.; Good, A. C. Analysis and Optimization of Structure-Based Virtual Screening Protocols. (3). New Methods and Old Problems in Scoring Function Design. *J. Mol. Graph. Model.* **2003**, *22*, 41–53.

(45) Boström, J. Reproducing the Conformations of Protein-Bound Ligands: A Critical Evaluation of Several Popular Conformational Searching Tools. *J. Comput.-Aided Mol. Des.* **2001**, *15*, 1137–1152.

(46) Good, A. C.; Cheney, D. L. Analysis and Optimization of Structure-Based Virtual Screening Protocols (1): Exploration of Ligand Conformational Sampling Techniques. *J. Mol. Graph. Model.* **2003**, *22*, 23–30.

(47) Chang, G. G.; W. C.; Still, W. C. An Internal Coordinate Monte Carlo Method for Searching Conformational Space. *J. Am. Chem. Soc.* **1989**, *111*, 4379–4386.

(48) Still, W. C.; Tempczyk, A.; Hawley, R. C.; Hendrickson, T. Semianalytical Treatment of Solvation for Molecular Mechanics and Dynamics. *J. Am. Chem. Soc.* **1990**, *112*, 6127−6129.
(49) Mohamadi, F. R.; Richards, N. G. J.; Guida, W. C.; Liskamp, R.; Lipton, M.; Caufield, C.; Chang, G.; Hendrickson, T.; Still, W. C. MacroModel−an Integrated Software System for Modeling Organic and Bioorganic Molecules Using Molecular Mechanics. *J. Comput. Chem.* **1990**, *11*, 440−467.
(50) Shenkin, P. S.; McDonald, D. Q. Cluster Analysis of Molecular Conformations. *J. Comput. Chem.* **1994**, *15*, 899−916.
(51) Wang, J.; Kollman, P. A.; Kuntz, I. D. Flexible Ligand Docking: A Multistep Strategy Approach. *Proteins* **1999**, *36*, 1−19.
(52) Zabell, A. P.; Post, C. B. Docking Multiple Conformations of a Flexible Ligand into a Protein Binding Site Using NMR Restraints. *Proteins* **2002**, *46*, 295−307.
(53) Clare, B. W. *MARTHA*; University of Western Australia: Crawley. Program available from the site http://www.chem.uwa.edu.au/research/bclare.
(54) Clare, B. W. Qsar of Benzene Derivatives: Comparison of Classical Descriptors, Quantum Theoretic Parameters and Flip Regression, Exemplified by Phenylalkylamine Hallucinogens. *J. Comput.-Aided Mol. Des.* **2002**, *16*, 611−633.
(55) Leach, A. R. *Molecular Modelling. Principles and Applications*; Pearson Educational Ltd: Harlow, 2001.
(56) Spiegel, M. R.; Liu, J. *Mathematical Handbook of Formulas and Tables*, 2nd ed.; McGraw-Hill: Singapore, 1999.
(57) Pellegrini, L. Role of Heparan Sulfate in Fibroblast Growth Factor Signaling: A Structural View. *Curr. Opin. Struct. Biol.* **2001**, *11*, 629−634.